daß $l_{x1}=l_{y1}=l_{x2}=l_{y2}=0$,
$l_{z1}=(m_2/M)^{1/2}$, $l_{z2}=-(m_1/M)^{1/2}$,
$Q=\sqrt{\mu}(r-l)$, $a_1=2\,l\sqrt{\mu}$ und $A=\mu\,l\,r$
ist und daher

$$H=\frac{1}{2\,\mu}\left(\frac{\hbar}{i}\right)^2\left\{\frac{1}{r^2}\left[\frac{1}{\sin\Theta}\frac{\partial}{\partial\Theta}\sin\Theta\,\frac{\partial}{\partial\Theta}+\frac{1}{\sin^2\Theta}\frac{\partial^2}{\partial\Phi^2}\right]+\frac{1}{r}\frac{\partial}{\partial r}\,r^2\frac{\partial}{\partial r}\frac{1}{r}\right\}+V. \quad (85)$$

Es muß hier noch beachtet werden, daß dieser Operator in einem Konfigurationsraum mit dem Volumenelement $d\tau=\sin\Theta\,d\Theta\,d\Phi\,dr$ definiert ist, während gewöhnlich [13] sphärische Koordinaten und das Volumenelement $d\tau=\sin\Theta\,d\Theta\,d\Phi\,r^2\,dr$ verwendet werden. Der zugehörige Hamilton-Operator lautet dann $\hat{H}=r^{-1}Hr$. Daraus ersieht man, daß Gl. (84) auf das richtige Ergebnis geführt hat.

Anm. b. d. Korr.: Die in Fußnote [17] genannte Arbeit von J. K. G. WATSON ist inzwischen in Mol. Phys. **19,** 465 [1970] erschienen. In dieser Arbeit wird unter anderem ebenfalls ein geschlossener Ausdruck für den Hamilton-Operator linearer Moleküle abgeleitet.

Strain Effects on the Tunneling Levels of KCl:Li

B. DISCHLER

Institut für Angewandte Festkörperphysik, Freiburg, Germany

(Z. Naturforsch. **25 a,** 1844—1855 [1970]; received 3 September 1970)

The effects of internal strains on the tunneling levels of KCl : Li are investigated quantitatively. The method, as developed in a preceding paper by TIMME, DISCHLER, and ESTLE [1], is further improved here. A reinterpretation is presented for two experimental results reported in the literature: the resonances in the phonon spectrometer curve and the specific heat (Schottky) anomaly. The agreement with these experiments and also with paraelectric resonance is good, if isotropic strains are assumed with an average energy of 20 GHz, corresponding to a stress of 30 ± 10 kp/cm². For the cube edge tunneling interaction a value of 10 GHz is derived.

Introduction

The interest in the system KCl:Li arises mainly from two facts: (i) the lithium ion is displaced from its substitutional lattice site in a ⟨111⟩ direction and (ii) tunneling occurs between these off-center positions. The physical properties of such a system differ in many respects from that of a normal (on-site) impurity. The phenomenon was discovered by the unusual thermal-conductivity [2], dielectric [3] and electrocaloric [4] behaviour of KCl:Li. Further evidence came from the observation of a specific-heat anomaly [5, 6] characteristic ultrasonic attenuation [7, 8], resonant phonon scattering [9], and paraelectric resonance with microwave [1a, 10, 11a] and far infrared [12] techniques. The original investigations were followed by refined or extended experiments with these types of measurements: thermal-conductivity [13, 14], dielectric behaviour [15], electrocaloric effect [16, 17], resonant phonon scattering [18, 19], paraelec-

Reprints request to Dr. B. DISCHLER, Institut für Angewandte Festkörperphysik, *D-7800 Freiburg i. Br.*, Eckerstraße 4.

[1] R. W. TIMME, B. DISCHLER, and T. L. ESTLE, a) Bull. Amer. Phys. Soc. **14,** 346 [1969]; b) Phys. Rev. **B 1,** 1610 [1970].
[2] F. C. BAUMANN, Bull. Amer. Phys. Soc. **9,** 644 [1964].
[3] H. S. SACK and M. C. MORIARTY, Solid State Comm. **3,** 93 [1965].
[4] G. LOMBARDO and R. O. POHL, Phys. Rev. Letters **15,** 291 [1965].
[5] R. F. WIELINGA, A. R. MIEDEMA, and W. J. HUISKAMP, Physica **32,** 1568 [1966].
[6] J. P. HARRISON, P. P. PERESSINI, and R. O. POHL, Phys. Rev. **171,** 1037 [1968].
[7] N. E. BYER and H. S. SACK, Phys. Rev. Letters **17,** 72 [1966].
[8] N. E. BYER and H. S. SACK, J. Phys. Chem. Solids **29,** 677 [1968].
[9] D. WALTON, Phys. Rev. Letters **19,** 305 [1967].
[10] G. HÖCHERL and H. C. WOLF, Phys. Letters **27 A,** 133 [1968].
[11] R. A. HERENDEEN and R. H. SILSBEE, a) Bull. Amer. Phys. Soc. **13,** 660 [1968]; b) Phys. Rev. **188,** 654 [1969].
[12] R. D. KIRBY and A. J. SIEVERS, Bull. Amer. Phys. Soc. **14,** 301 [1969].
[13] F. C. BAUMANN, J. H. HARRISON, R. O. POHL, and W. D. SEWARD, Phys. Rev. **159,** 691 [1967].
[14] P. P. PERESSINI, J. H. HARRISON, and R. O. POHL, Phys. Rev. **180,** 926 [1969].
[15] A. LAKATOS and H. S. SACK, Solid State Comm. **4,** 315 [1966].
[16] S. KAPPHAN and F. LÜTY, Solid State Comm. **6,** 907 [1968].
[17] R. O. POHL, V. L. TAYLOR, and W. M. GOUBAU, Phys. Rev. **178,** 1431 [1969].
[18] D. WALTON, in: Localized Excitations in Solids, R. F. WALLIS, Ed., Plenum, New York 1968.
[19] M. C. HETZLER and D. WALTON, Phys. Rev. Letters **24,** 505 [1970].

tric resonance [1b, 11b, 20], local mode infrared absorption [21], NMR quadrupole splitting [22, 23], and microwave to phonon conversion [24]. An up-to-date review article on "Tunneling states of defects in solids" has appeared recently [25].

In most interpretations the lithium has been assumed to be in an ideal host, at least at low lithium concentrations. However, from paraelectric resonance results it was concluded [1, 11b] that in a real crystal the off-center lithium experiences large perturbations from internal strains. Results of detailed numerical calculations on the effects of internal strains will be presented in this paper. The general method will be described, and the case of zero external electric field and zero applied stress will be treated. Subsequent parts [26] will deal with strain effects in paraelectric resonance spectra.

The first section define the properties of the off-center lithium and especially its response to uniaxial stress. In the second section it is shown, how the random internal strains can be approximated by uniaxial strain in selected directions with subsequent averaging. In section three the distribution of energy levels in the presence of internal strains is computed * and compared with experimental observations. The discussion in section four will show, that the present knowledge is sufficient to explain most of the observations, but further investigations are necessary to obtain complete understanding.

1. Model Hamiltonian for the Off-Center Lithium

The basic model explaining the physical properties of the off-center lithium has been established during the past years. Minima in the potential surface are found in the eight ⟨111⟩ directions, both experimentally [7, 8, 16] and theoretically [27, 28]. In Fig. 1 the location of the eight ⟨111⟩ minima is indicated schematically, using the numbers 1 through 8. From

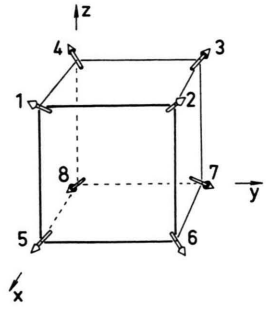

Fig. 1. Schematic picture showing the location of the eight ⟨111⟩ potential minima for the lithium ion in KCl. The numbering of the individual states and the orientation of the electric dipole moment are indicated.

a classical point of view, the lithium will be located in one particular minimum, and in the quantum mechanical treatment this will be called an "individual state". The displacement from the cubic lattice site to the ⟨111⟩ off-center position lowers the point symmetry from O_h to C_{3v}. Therefore an electric dipole moment and an elastic moment are associated with each individual state.

Experimental values quoted for the electric dipole moment range from 2.53 to 4.0 D (see Table 1). The elastic moment can only be estimated indirectly from the results of the ultrasonic measurements [8] or the Li^7 NMR, where uniaxial stress induces quadrupole splittings [22, 23].

Mapping out the potential surface [28] shows, that the off-center minima are separated by barriers, which are low enough to allow interactions between the individual states. The usual way to treat these interactions is the tunneling approximation [29–32], already familiar from the inversion splitting of the NH_3 molecule. In this approximation phenomenological parameters are introduced, which allow one to construct the energy matrix without specifying the basis functions. The latter would have to be eigen-functions for the individual states. It has been

[20] D. Blumenstock, R. Osswald, and H. C. Wolf, Z. Physik **231**, 333 [1970].
[21] B. P. Clayman, I. G. Nolt, and A. J. Sievers, Phys. Rev. Letters **19**, 111 [1967].
[22] D. W. Alderman and R. M. Cotts, a) Bull. Amer. Phys. Soc. **13**, 1672 [1968]; b) Phys. Rev. **B 1**, 2870 [1970].
[23] W. D. Wilson and M. Blume, J. Phys. Chem. Solids **29**, 1167 [1968].
[24] D. J. Channin, V. Narayanamurti, and R. O. Pohl, Phys. Rev. Letters **22**, 524 [1969].
[25] V. Narayanamurti and R. O. Pohl, Rev. Mod. Phys. **42**, 201 [1970].
[26] B. Dischler, to be published.

* Use was made of the IBM 7040 computer of the Rechenzentrum der Universität Freiburg i. Br.
[27] R. J. Quigley and T. P. Das, a) Phys. Rev. **164**, 1185 [1967], and References given therein; b) Phys. Rev. **177**, 1340 [1969].
[28] W. D. Wilson, R. D. Hatcher, R. Smoluchowski, and G. J. Dienes, Phys. Rev. **184**, 844 [1969].
[29] J. W. Corbett, Amer. J. Phys. **31**, 521 [1963].
[30] H. B. Shore, Phys. Rev. **151**, 570 [1966].
[31] a) S. P. Bowen, M. Gomez, J. A. Krumhansl, and J. A. D. Matthew, Phys. Rev. Letters **16**, 1105 [1966]; b) M. Gomez, S. P. Bowen, and J. A. Krumhansl, Phys. Rev. **153**, 1009 [1967].
[32] T. L. Estle, Phys. Rev. **176**, 1056 [1968].

Method	Conditions	$p(Li^7)$[a] (Debye)[b] p_{eff}	p_0	$p(Li^6)$[a] (Debye)[b] p_{eff}	p_0	Ref.[c]
dielectric	$< 40°K$	≈ 2	≈ 1	—	—	3
paraelectric resonance	7 ppm Li 4.2°K	8.6	4.0	—	—	10
paraelectric resonance	1°K	7.0	3.2	—	—	32
paraelectric resonance	7 ppm Li 1.3°K	6.0	2.8	—	—	1
paraelectric resonance	4.4 ppm Li 4.2°K	5.6 ± 0.2	2.6 ± 0.1	5.6 ± 0.2	2.6 ± 0.1	11b
paraelectric resonance	1 ppm Li 2°K	6.3 ± 0.3	2.9 ± 0.15	—	—	22
paraelectric infrared absorption		5.47	2.53	5.47	2.53	12
electrocaloric	150 ppm Li $10^{-1}-1°K$	5.5	2.54	—	—	1
electrocaloric	25 ppm Li 1.37°K	6.2 ± 0.6	2.9 ± 0.3	—	—	16
Schottky anomaly	12 ppm Li 0.1–1°K	5.95 ± 0.54	2.75 ± 0.25	—	—	6
theory	2°K	11.2	5.15	11.2	5.15	22b

[a] p_0 is the local dipole moment, corrected with the Lorentz field, where $p_0 = 0.462\ p_{eff}$.
[b] The relation between Debye and eÅ units is: 1 eÅ = 4.8 D.
[c] Ref. numbers according to this paper.

Table 1. Electric dipole moment for off-center Li in KCl.

pointed out [33, 34] that the vibronic coupling between a charged defect and the lattice is important. This is in agreement with the large displacements calculated for the lattice ions in the neighbourhood of the lithium [27]. It is therefore not surprising to find an effectively small interaction between the individual states and a negligible overlap. For the lithium in the ⟨111⟩ off-center position, the eightfold degenerate ground state is split into four tunneling levels which transform like A_{1g}, T_{1u}, T_{2g} and A_{2u}. These tunneling levels are equidistant if the reasonable assumption is made, that tunneling interactions occur only between neighbouring potential wells. This equidistance of the levels has been used in the interpretation of all Li^7 experiments, except one [20], and a spacing in the range from 18 to 24.6 GHz has been obtained (see Table 2).

The energy matrix can now be set up, where the numbering of the individual states is given in Fig. 1. The electric field F and the stress field S appear in the diagonal elements, which take the following form:

$$
\begin{aligned}
H_{11} &= p(-F_x+F_y-F_z)+q(\ \ S_{xy}-S_{xz}+S_{yz}),\\
H_{22} &= p(-F_x-F_y-F_z)+q(-S_{xy}-S_{xz}-S_{yz}),\\
H_{33} &= p(\ \ F_x-F_y-F_z)+q(\ \ S_{xy}+S_{xz}-S_{yz}),\\
H_{44} &= p(\ \ F_x+F_y-F_z)+q(-S_{xy}+S_{xz}+S_{yz}),\\
H_{55} &= p(-F_x+F_y+F_z)+q(\ \ S_{xy}+S_{xz}-S_{yz}),\\
H_{66} &= p(-F_x-F_y+F_z)+q(-S_{xy}+S_{xz}+S_{yz}),\\
H_{77} &= p(\ \ F_x-F_y+F_z)+q(\ \ S_{xy}-S_{xz}+S_{yz}),\\
H_{88} &= p(\ \ F_x+F_y+F_z)+q(-S_{xy}-S_{xz}-S_{yz}).
\end{aligned}
\qquad (1)
$$

All contributions which merely shift the total energy are suppressed.

The quantities F_x, F_y, and F_z are the components of the electric field in the x, y, and z direction. If the energy is measured in GHz and F is meaured in kV/cm the coefficient p is given by

$$p = 0.627\ p_0\ \text{GHz}\cdot\text{cm/V}$$

[33] H. B. Shore, Phys. Rev. Letters **17**, 1142 [1966].

[34] R. Sittig, a) Phys. Stat. Sol. **34**, K 189 [1969], and to be published; b) Dissertation, Frankfurt 1970.

Method	Conditions[a]	Li^7 (GHz)[b]	Li^6 (GHz)[b]	Ref.[c]
dielectric		$\Delta = 22.5$	—	d
dielectric	2.6 ppm Li 4—30° K	$\Delta = 24.3$	—	15
paraelectric resonance	1°K	$\Delta = 21$	—	32
paraelectric resonance	4.4 ppm Li 4.2°K	$\Delta = 23.1 \pm 0.9$	$\Delta = 32.1 \pm 1.2$	11b
paraelectric resonance	7 ppm Li 1.3°K	$\Delta \geqq 20$[e]	—	1
paraelectric resonance	1 ppm Li 2°K	$\Delta_1 = 35.4 \pm 3$ $\Delta_2 = 58.0$ $\Delta_3 = 67.8$	—	20
phonon spectrometer	1.2 ppm Li 0.47°K	$\Delta_1 = 18 \pm 3$ $\Delta_2 = 39 \pm 3$ $\Delta_3 = 66 \pm 3$ $(\Delta = 22)$	—	9
phonon spectrometer	0.09 ppm Li 0.34°K	$\Delta_1 = 21 \pm 3$ $\Delta_2 = 42 \pm 3$ $\Delta_3 = 66 \pm 3$ $(\Delta = 22)$	—	18
phonon spectrometer	3 ppm Li 1.0°K	—	$\Delta_1 = 31.5$ $\Delta_2 = 52.5$ $\Delta_3 = 82.5$	19
thermal conductivity	0.5—1°K	$\Delta_{av} \approx 10$	—	2
thermal conductivity	44 ppm Li 0.05—1°K	$\Delta_{av} = 36$	$\Delta_{av} = 52.2$	13, 14
Schottky anomaly	18 ppm Li 0.1—1°K	$\Delta = 24.6$	$\Delta = 34.5$	6
this paper (see Table 3)	0.1—100 ppm 1—4°K	$\Delta = 21.3$[e]	—	—

[a] As far as given in the literature.
[b] 30 GHz correspond to 1 cm^{-1}.
[c] Ref. numbers according to this paper, [d] see below.
[d] BOGARDUS and SACK, Bull. Amer. Phys. Soc. **11**, 229 [1966].
[e] For strain-broadened levels, $\Delta \geqq |2\eta|$.

Table 2. Spacing (Δ without subscript) between tunneling levels of KCl : Li. Δ_1, Δ_2, and Δ_3 denote the separation from the ground state and Δ_{av} is the weighted average of Δ_1, Δ_2, and Δ_3.

where p_0 is the local electric dipole moment in Debye units. The number 0.627 is the product of $\cos(54.7°) = 0.577$ (for $\langle 111 \rangle$ dipoles), $(\varepsilon_{KCl} + 2)/3 = 2.16$ (Lorentz field correction) and a factor 0.503 for conversion of units ($1\,D/h = 0.503 \cdot 10^6$ cm/V $\cdot$ sec $= 0.503$ GHz $\cdot$ cm/kV).

Since the KCl:Li interacts only with stress of T_{2g} symmetry [8], the uniaxial stress is expressed in the components S_{xy}, S_{xz}, and S_{yz} (see Appendix I). If S is measured in kp/cm^2 the coefficient q is given by

$$q = 35.8\, q_0 \ \text{GHz} \cdot \text{cm}^2/\text{kp}$$

where $3\,q_0 = (\lambda_{\parallel} - \lambda_{\perp})$ is the dimensionless shape factor [8]. The number 35.8 is the product of $2.42 \cdot 10^{-22}$ cm^3 ($= V_0$, volume of the primitive cell in KCl) and a factor $1.48 \cdot 10^{23}$ for conversion of units

$$(1\ \text{cm}^3/\text{h} = 1.48 \cdot 10^{32}\ \text{cm}^2/\text{kp} \cdot \text{sec} = 1.48 \cdot 10^{23}\ \text{GHz} \cdot \text{cm}^2/\text{kp}).$$

The tunneling interaction appears in the 28 off-diagonal elements:

$$\begin{aligned} &H_{12} = H_{14} = H_{15} = H_{23} = H_{26} = H_{34} = H_{37} = H_{48} = H_{56} = H_{58} = H_{67} = H_{78} = \eta\,, \\ &H_{13} = H_{16} = H_{18} = H_{24} = H_{25} = H_{27} = H_{36} = H_{38} = H_{45} = H_{47} = H_{57} = H_{68} = \mu\,, \\ &H_{17} = H_{28} = H_{35} = H_{46} = \nu\,. \end{aligned} \tag{2}$$

Where η has been named the "cube edge", μ the "cube face" and ν the "body diagonal" tunneling, taking into account that there exist three different geometrical configurations (see Fig. 1). In a classical picture the three parameters would correspond to a reorientation of the electric dipole through an angle of 71° for η, 109° for μ, and 180° for ν. Note that according to the tunneling approximation overlap matrix elements are omitted in Eq. (2).

In the absence of an electric field and of stress the diagonal elements of Eq. (1) vanish and the eigenvalue problem has the well known solution [31]:

$$\begin{aligned} E(A_{1g}) &= 3\eta + 3\mu + \nu, \\ E(T_{1u}) &= \eta - \mu - \nu, \\ E(T_{2g}) &= -\eta - \mu + \nu, \\ E(A_{2u}) &= -3\eta + 3\mu - \nu. \end{aligned} \tag{3}$$

Since η, μ, and ν can only assume negative values, the totally symmetric A_{1g} state is always lowest. In the following the parameters μ and ν are assumed to be zero, which corresponds to equidistant levels at 3η, η, $-\eta$, and -3η. This is believed to be true for KCl:Li for the following reasons: (i) the experimental results, especially from the phonon spectrometer [9] suggest equidistant energy levels, (ii) the theoretical calculations on the potential surface [27, 28] have shown that minima, which are only slightly shallower than the ⟨111⟩ minima exist for ⟨110⟩ displacements (see Fig. 2); the "cube edge" interaction should therefore be highly favoured by low barriers. It may also be mentioned that for the strain effects to be studied here the simplest level scheme is sufficient to arrive at the essential conclusions.

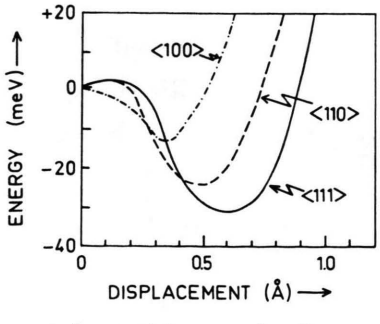

Fig. 2. Theoretical potential curves after QUIGLEY and DAS [27] for displacements of the lithium ion from the KCl lattice site along the ⟨100⟩, ⟨110⟩, and ⟨111⟩ axes. The lowest minimum is found for ⟨111⟩ displacements. The curves were obtained [27a] with the room temperature lattice parameter of 3.147 Å. At 2 °K the lattice parameter is 3.117 Å and the ⟨111⟩ minimum is found [27b] at 0.45 Å displacement with a depth of only 12 meV.

In a more accurate description the tunnel parameter η must be taken stress dependent. Consequently three different "cube edge" tunnelings η_x, η_y, and η_z have to be used, if the cube of Fig. 1 becomes distorted by uniaxial stress. Such effects are measurable as has been shown by recent paraelectric resonance experiments, where spectra have been taken under ⟨100⟩ uniaxial stress [20]. Also from the theoretical point of view the tunneling interaction should be sensitive to stress, since the calculations on the potential surface have lead to the prediction [27b] that for a hydrostatic pressure of $7 \cdot 10^3$ kp /cm² the off-center minima vanish (η would have to diverge to infinity in the tunneling approximation). If this dependence of η on stress is taken into account by a linear approximation, Eqs. (2) must be changed to:

$$\begin{aligned} H_{14} = H_{23} = H_{58} = H_{67} &= \eta[1 + \alpha S_x - \beta(S_y + S_z)] = \eta_x, \\ H_{12} = H_{34} = H_{56} = H_{78} &= \eta[1 + \alpha S_y - \beta(S_x + S_z)] = \eta_y, \\ H_{15} = H_{26} = H_{37} = H_{48} &= \eta[1 + \alpha S_z - \beta(S_x + S_y)] = \eta_z, \end{aligned} \tag{4}$$

where S_x, S_y, and S_z are the stress components in the x, y, and z direction. The coefficient α can be estimated from a fit to the experiment under uniaxial stress [20], whereas β is unknown.

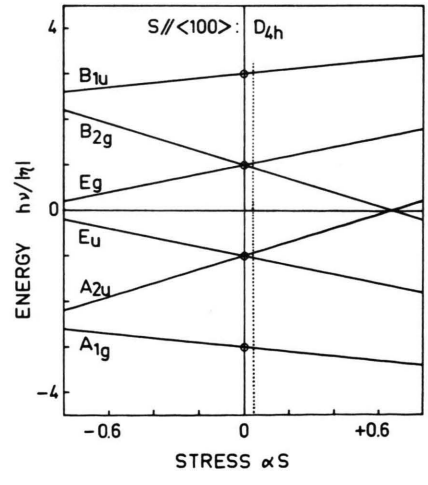

Fig. 3. Energy levels of KCl : Li as a function of ⟨100⟩ uniaxial stress. Eq. (4) with the assumed ratio $\beta S = \alpha S/4$ has been used. The dotted line indicates the stress value $\alpha S = 0.04$ which is later used in Fig. 6.

With Eqs. (1) and (4) the energy matrix is now complete. With $F = 0$ and $S \neq 0$ the influence of uniaxial stress on the energy levels of the tunneling states can be calculated. This has been done for the directions ⟨100⟩, ⟨111⟩, and ⟨110⟩, and the re-

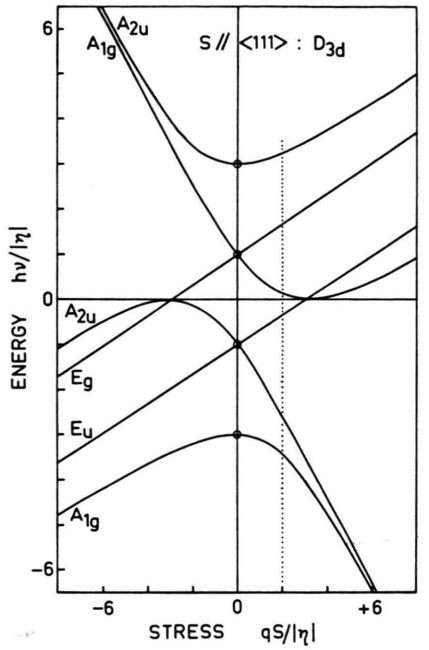

Fig. 4. Energy levels of KCl : Li as a function of ⟨111⟩ uniaxial stress. The effect of the stress on the tunneling is included with the assumed ratio $\alpha S=0.02\, q S/|\eta|$ and $\beta S=\alpha S/4$. The dotted line indicates the stress value used in Fig. 6. Note, that in Fig. 7 of Ref. [22b] the crossovers near $q S/|\eta| = \pm 3$ are missing, contrary to simple rules, which predict the high strain limit.

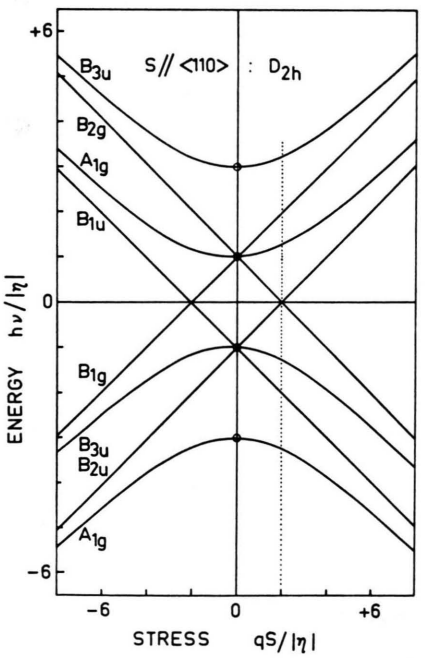

Fig. 5. Energy levels of KCl : Li as a function of ⟨110⟩ uniaxial stress. The effect of the stress on the tunneling is included with the assumed ratio $\alpha S=0.02\, q S/|\eta|$ and $\beta S=\alpha S/4$. The dotted line indicates the stress value used in Fig. 6.

sults are shown in Figs. 3, 4, and 5. In the angular dependence diagram of Fig. 6 the stress direction is rotated in a (110) plane and the magnitude of the stress is kept constant. Figures 3 through 6 demonstrate the effectiveness of internal strains in broadening the tunneling levels.

In these figures energy and stress are given in normalized (dimensionless) units in order to make the diagrams independent of the actual values for η, q, α, and β. This could be fully accomplished for Fig. 3, which is determined by η, α, and β alone. However, in Figs. 4, 5, and 6 the stress normalization is performed only with respect to the dominant elastic effects, which are represented by q. For the changes in the tunneling parameters with stress, which are included in these diagrams, a fixed ratio relative to the elastic effects had to be chosen. Here the same ratio as in Sect. 3 has been used, namely

$$\alpha S = 0.02\, q S/|\eta| \quad \text{and} \quad \beta S = \alpha S/4\,.$$

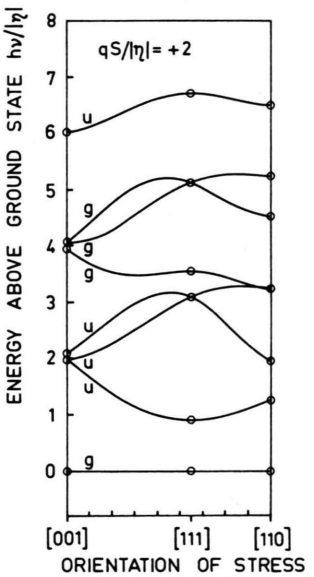

Fig. 6. Energy levels of KCl : Li relative to the ground state as a function of stress orientation in the (110) plane for $q S/|\eta| = +2$, $\alpha S=0.04$, and $\beta S=0.01$. The overall symmetry is C_s.

2. Internal Strains

2.1. Direction and Magnitude of Strains

The host material KCl has crystalline imperfections (dislocations etc.) which give rise to internal strains. The energy levels of the off-center lithium

are modified by these strains (cf. Fig. 6). If the strains occur at random, which is a reasonable assumption, the distribution of strain directions will be isotropic. In the present model calculation this is simulated by selecting 13 different directions with appropriate statistical weights (see Appendix II).

The magnitude of the strain follows a statistical distribution, which is not known in detail, and which may differ from sample to sample. In a previous calculation [1] nine different magnitudes of S were assumed, which implies assumptions on the distribution of S and increased computational effort. In the present calculation only two values (viz. an average magnitude, taken positive and negative) are used, and this procedure can be justified as follows: Almost identical results were obtained with nine different magnitudes of S or with one average magnitude in all test cases where comparisons were made. This is not too surprising, since by changing the stress orientation the different components of S assume all values between an upper and lower limit, which is determined by the magnitude of S.

2.2. The Moment Method

In a calculated spectrum, the transitions will at first be delta functions. Consideration of the natural linewidth and the spectrometer resolution would lead to lines which are still sharper than the observed broad signals. The experimentally determined relaxation time for KCl:Li at 1.4 °K is $1 \cdot 10^{-8}$ sec from electrocaloric measurements [16] and $1 \cdot 10^{-9}$ sec from paraelectric resonance [11]. The corresponding halfwidth is of the order of 0.16 GHz. In the present calculation on strain broadening it would be possible to replace each line by a Gaussian of appropriate width. However, this introduces at least one additional parameter for the average width. This can be avoided by a procedure, which is a special version of the well known moment method. The delta functions occur in obvious groupings. Each such group is treated as one signal, characterized by its position R and its width W. For the replacement of a group of delta functions by an envelop of Gaussian shape, the following expressions can be used

$$R = \langle R^1 \rangle = (\sum_k R_k I_k) / \sum_k I_k , \qquad (5\,a)$$

$$W = (\sum_k | R - R_k | \cdot I_k) / \sum_k I_k \qquad (5\,b)$$

where R_k and I_k are the position and the intensity of the k-th δ-function within the group. A convenient shape parameter is the width at half height $2 W_h$, which is related to W by the approximation

$$2 W_h \approx 3 W \qquad (5\,c)$$

where the factor 3 was obtained by application of Eq. (5 b) to a Gaussian.

3. Comparison with Experiment

Lithium has two isotopes with natural abundance of 93% (Li^7) and 7% (Li^6). In Tables 1 and 2 results on Li^6 are from samples, where this isotope had been enriched to 99%. There is no measurable isotope effect for the electric dipole moment, but a 40% increase of the tunnel splitting for Li^6. A far infrared absorption has been observed [21] at 40 cm^{-1} for Li^7 and at lower frequency for Li^6, and has been assigned to the first excited vibrational state [12]. A theoretical explanation for the sign and the magnitude of the isotope effects has not been given so far. The present calculations have been performed for the isotope Li^7, but it is expected that they are representative for the isotope Li^6 too.

With the formalism developed so far, the model calculation can now be performed. An actual value must be used for the average elastic energy, $q S$. The paraelectric resonance is very sensitive to strains [1, 11, 26] and a fit has been made which yielded [26] $q S/|\eta| = 2 \pm 1$. The remaining parameters of the Hamiltonian are more or less fixed by the published experimental results. The following set is used in the present calculation:

$$\eta = -10 \text{ GHz}, \quad \eta\,\alpha\,S = \mp 0.40 \text{ GHz},$$
$$q S = \pm 20 \text{ GHz}, \quad \eta\,\beta\,S = \mp 0.10 \text{ GHz}. \qquad (6)$$

The effects connected with the parameters α and β are very small, but for completeness they have been included. The values for αS and βS are derived as follows: The dimensionless shape parameter

$$3 q_0 = (\lambda_{\parallel} - \lambda_{\perp})$$

has been determined in the ultrasonic experiment [8] with the result $3 q_0 = +0.062 \pm 0.009$, and using the quadrupole splitting in the Li^7 NMR [22] with the result $3 q_0 = \pm 0.042 \pm 0.003$. Taking an average q_0, the stress corresponding to $q S = 20$ GHz is $S = 30 \pm 10$ kp/cm². With $\alpha = 1.3 \cdot 10^{-3}$ cm²/kp from a fit [26] to the paraelectric resonance under uniaxial $\langle 100 \rangle$ stress [20] the value $\eta\,\alpha\,S = -0.40$ GHz is obtained. The ratio $\beta = \alpha/4$ was chosen by considering the elastic deformation of a KCl cube under uniaxial stress.

Levels for $S=0$ (GHz)	Levels for $qS/\|\eta\| = -2$ (GHz)	$qS/\|\eta\| = +2$ (GHz)	Statist. weight per level	Center of grav. (GHz)	Density of states for $\|qS/\eta\| = 2$ Halfwidth $2W_h$ (GHz)	Statist. weight
60 (A_{2u})	59.6	60.4	27	64.0	6.4	200
	66.1	67.3	28			
	64.2	65.2	45			
40 (T_{2g})	39.4; 39.4; 40.4	39.6; 40.6; 40.6	27	42.7	19.7	600
	35.3; 35.3; 57.7	35.6; 51.4; 51.4	28			
	32.3; 44.0; 52.3	32.5; 45.5; 52.5	45			
20 (T_{1u})	19.2; 20.2; 20.2	19.8; 19.8; 20.8	27	21.3	18.1	600
	15.5; 15.5; 31.1	8.8; 31.1; 31.1	28			
	12.0; 20.3; 32.0	12.7; 19.7; 32.7	45			
0 (A_{1g})	0	0	100	0	0	200

Table 3. Energy level distribution for KCl : Li^7. Columns 5, 6, and 7 are obtained from columns 2, 3, and 4 by application of the moment method (see Sect. 2.2).

The result obtained with Eqs. (1), (4), (6) in the absence of external fields (i. e. $F=0$) is shown in Table 3. It can be compared directly with the phonon spectrometer results, and indirectly with the data on the specific heat anomaly.

3.1. Phonon Spectrometer Experiment

In contrast to the relatively sharp tunneling levels, which the lithium ions might have in an ideal KCl host under the influence of relaxation only, considerable broadening occurs in the real host, as shown in Fig. 7. The calculated curve (Fig. 7 a) shows the density of states for an ensemble of lithium ions in KCl. The experimental curves (Fig. 7 b – d) reproduce results of WALTON [9, 18]. His "phonon spectrometer" can be sketched only briefly here. In addition to the lithium the sample contains $5 \cdot 10^{16}$ paramagnetic R-centers [35]. In an applied magnetic field the Zeeman splitting of the R-centers is tuned to a single Larmor frequency between 0 and 80 GHz, where $\nu_L = g\beta H$. The R-centers remove from the phonon spectrum a small band around ν_L, and these missing phonons ar detected indirectly by a decrease in thermal conductivity. Therefore, the change in thermal conductivity as a function of magnetic field is representative for the phonon distribution in the sample. For KCl:Li this qualitative "phonon spectrum" is structured, with extrema in the neighbourhood of 20, 40, and 65 GHz (see Fig. 7). The conclusion was [9] that resonant phonon scattering by the lithium tunneling levels is responsible for these resonance dips. This was later confirmed by the observation of an isotope effect [19]. For isotopically enriched Li^6 the resonance dips ocur at 40% higher frequencies (see Table 2).

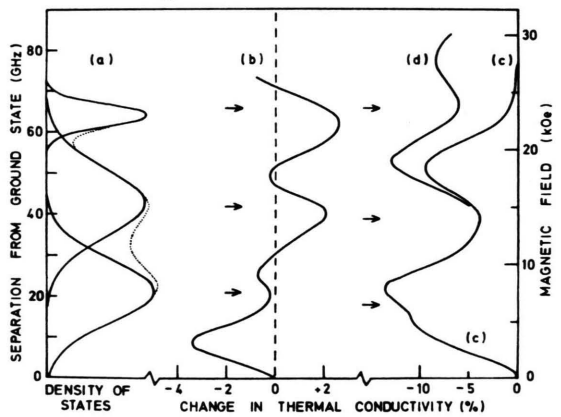

Fig. 7. Comparison of calculated density of states (a) (cf. Table 3, columns 5, 6, 7) with the experimental phonon spectrometer curves (b – d) of WALTON [9, 18] for KCl : Li. Curve (b) is for 0.09 ppm Li at 0.34 °K. Curves (c, d) are for 1.2 ppm Li at 0.47 °K (c) and 0.57 °K (d). Curve (a) is for Li^7, neglecting anomalous lithium. Curves b, c, d are for natural isotopic mixture with 93% Li^7. The arrows indicate the experimental resonance positions, quoted by WALTON [9, 18].

The agreement between calculated and experimental curves is satisfactory. In order to characterize the experimental difficulties, two observations may be mentioned: (i) the relative depth of the extrema is sample dependent in a way which is not understood [18], (ii) the curve in Fig. 7 b extends into regions of increased thermal conductivity, contrary

[35] The *R*-center is formed by three adjacent *F*-centers, and is known for its degenerate ground state and the very large spin phonon interaction, see e. g. D. C. KRUPKA and R. H. SILSBEE, Phys. Rev. **152**, 816 [1966].

to expectations based on the simple picture given above; in an improved treatment [36], the increase in thermal conductivity can be explained.

3.2. *Schottky Anomaly*

Measurements on the specific heat of KCl:Li by WIELINGA, MIEDEMA, and HUISKAMP [5] and by HARRISON, PERESSINI, and POHL [6] have revealed a pronounced peak (Schottky anomaly) in the range 0.5 to 1 °K. Figure 8 shows calculated curves together

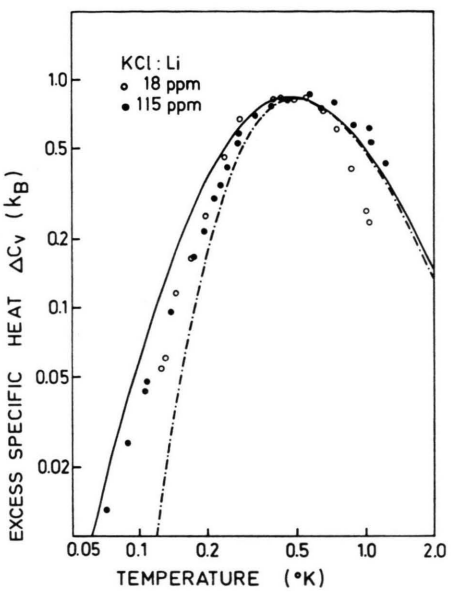

Fig. 8. Comparison of calculated Schottky anomaly for KCl:Li with the experimental results of HARRISON, PERESSINI and POHL [6], where the contribution of the host has been substracted. Open circles are from the 18 ppm sample "A" and closed circles are from the 115 ppm sample "G", both having natural isotopic mixture of 93% Li^7 and 7% Li^6. The solid curve is from the present calculation, and the dash-dot curve is calculated after HARRISON et al. [6].

with the experimental points of HARRISON et al. [6] for their samples "A" and "G" (18 and 115 ppm Li, resp.). For higher lithium concentrations the points do no longer fall on the same curve, due to broadening and a shift of the Schottky anomaly peak to higher temperatures. The dashed curve is the best fit of HARRISON et al. [6], calculated for three sharp levels with 24.6 GHz spacing and under the assumption that only 53% of the chemically identified lithium contributes to c_v. The solid curve is from the present calculation (see Appendix III). The agreement with the experimental points is very satisfactory, especially for the lowest temperatures. This solid curve takes into account the internal strains, and as an additional improvement contains the full 100% of the lithium, found in the spectrochemical analysis. This was accomplished by postulating contributions from two different types of lithium. While most of the Li ions are at "normal" sites, some are in an "anomalous" environment, e. g. close to a dislocation line. The energy level scheme for the "anomalous" lithium is derived in Appendix IV. A spacing of 24 GHz has been assumed in order to fit the experimental points. The large difference in peak height for normal and anomalous lithium (see Appendix IV) allows an estimate of the respective percentages. For the two concentrations, 18 and 115 ppm, the same result of 60% normal and 40% anomalous lithium is obtained.

The possibility, that one deals with two types of lithium has been mentioned previously [6, 7, 11b], however, the inclusion of such a situation in the calculations has not been attempted before. Usually the Li^6 isotope is neglected [6] in the interpretation of experiments on the natural isotopic mixture. The present calculation considers contributions from both isotopes, where $\eta(Li^6) = -14$ GHz has been assumed.

The solid curve in Fig. 8 has been obtained by summation over the following four contributions: (i) normal Li^7 with the strain broadened energy level distribution of Table 3, (ii) anomalous Li^7 with 24 GHz spacing, (iii) normal Li^6, for which the energies of Table 3 were multiplied by 1.4, and (iv) anomalous Li^6 with 34 GHz spacing. For example, the total value 0.826 k_B at 0.5 °K is the sum of (i) 0.605, (ii) 0.162, (iii) 0.047, and (iv) 0.012. Note that (i) is the dominant contribution and consequently the peak position of the Schottky anomaly is essentially determined by the tunneling parameter $\eta = -10$ GHz of the normal Li^7 ions.

4. Discussion

Evidence for considerable strain effects has been derived previously from paraelectric resonance results [1, 11b] and also from residual line width in the Li^7 NMR [22]. The phonon spectrometer and specific heat measurements are less conclusive in this respect, however, the agreement with the calculated data has been improved by the assumption of internal strains. It is an important feature of the present calculation that the strain effects are independent of

[36] D. WALTON, Phys. Rev. **B 1**, 1234 [1970].

Li concentration up to moderately high concentrations (120 ppm, approx.). In contrast HARRISON et al.[6] and POHL et al.[17] assumed sharp levels for low concentrations and stress broadening for high concentrations (75 ppm and above). However the paraelectric resonance results, mentioned above, show that the strain effects remain unchanged down to the lowest Li concentrations (0.1 ppm).

Close inspection of Fig. 7 a, b shows that the observed halfwidth is smaller than calculated near 40 GHz and larger than calculated near 60 GHz. Since long wavelength acoustical phonons are involved, the selection rules for the ideal host would allow A_{1g} to T_{2g} transitions, whereas A_{1g} to T_{1u} and A_{1g} to A_{2u} transitions would be forbidden. In the real crystal these selection rules are relaxed by inhomogeneous internal strains and possibly by internal electric fields. The observed differences in halfwidth would occur if the formerly allowed transitions near 40 GHz become partially forbidden as they are shifted from the center to the flanks, and the formerly forbidden transitions near 60 GHz become more and more allowed as they are shifted. Further measurements are necessary to reach conclusions about inhomogeneous internal strains and random internal electric fields.

From the measured peak height of the Schottky anomaly it was estimated that 40% of the chemically identified lithium is at anomalous sites in the crystal. In this connection some peculiar observations may be mentioned: (i) KCl:Li samples kept at room temperature undergo an "aging" effect[8, 13, 17], where the fraction of normal or "free" Li ions decreases at a rate of 30% per year[13, 17]. At the same time the number of dislocation lines increases[8], (ii) in paraelectric cooling experiments with ⟨111⟩ oriented field the observed low-temperature low-field cooling exceeds the calculated value by a factor of two[17], (iii) under certain conditions the behaviour of KCl:Li is irreversible in the sense that the properties of a sample depend on its thermal and electrical "history". For electrocaloric experiments this is observed[17] for fields above 10 kV/cm and temperatures below 0.5 °K. In paraelectric resonance a hysteresis type behaviour has been found[11] in ⟨100⟩ spectra taken at 23 and 25 GHz and at 4.2 °K. This effect has its onset at 10 kV/cm and saturates above 30 kV/cm.

The explanation for the aging effect (i) could be, that some of the Li ions which are originally at normal sites are later found at anomalous sites. The number of dislocation lines increases parallel with the aging[8], but in addition some Li ions may be "trapped" at anomalous sites during their diffusion at room temperature.

With respect to (ii) it should be mentioned, that the cooling was calculated with the assumption of sharp levels with 24.6 GHz spacing. A corresponding calculation for strain broadened levels has not been performed, however, following qualitative arguments, an increase in low-temperature low-field cooling is expected.

For the observations under (iii) no explanation has been offered so far. The response of the anomalous lithium and its environment to an external electric field is not known. The hysteresis behaviour suggests the existence of an internal electric field[11] close to each dislocation line and a possible reorientation of the anomalous lithium relative to this internal field if the external field exceeds 10 kV/cm. If this interpretation can be confirmed, it would be interesting to investigate the mechanisms of the reorientation.

Some discussion has been devoted to a possible ferro- or antiferroelectric ordering at sufficiently low temperatures and high enough Li concentrations[6, 8, 13, 14, 17, 37]. In samples with lithium concentrations of 250 ppm and above ferroelectric type polarisation behaviour has been observed in high electric fields[37] (see also [25]), however all attempts to observe a ferroelectric transition at the predicted temperatures have been unsuccessful so far. The reason could be, that random internal strains with their average energy of 20 GHz dominate over the electric dipole-dipole interaction, which reaches 20 GHz only at the very high concentration of about 500 ppm[25]. Also it must be kept in mind, that the interaction of the elastic moments of the off-center lithium tries to establish an "antiferroelastic" order[8]. Preliminary estimates[8] do not rule out the possibility that elastic and electric interaction energies are of similar magnitude. However, the consequences of such a competition have not been investigated theoretically.

Acknowledgements

The author would like to acknowledge many valuable discussions with Prof. T. L. ETSLE. The author is grateful to Rice University, Houston, Texas, for hospitality during 1968/69.

[37] A. T. FIORY, Bull. Amer. Phys. Soc. **14**, 346 [1969].

Appendix I

Decomposition of Uniaxial Stress into T_{2g} Components

If the x, y, and z components of the uniaxial stress are given by S_y, S_y, and S_z, the corresponding values for the T_{2g} components S_{xy}, S_{xz}, and S_{yz} to be used with Eq. (1) are given by

$$S_{xy}=S_x\cdot S_y/|S|\,,\quad S_{xz}=S_x\cdot S_z/|S|\,,\quad S_{yz}=S_y\cdot S_z/|S|\,.$$

All three T_{2g} components vanish for uniaxial stress in a $\langle 100\rangle$ direction, i. e. $S_x\neq 0$, $S_y=S_z=0$. For $\langle 111\rangle$ stress $S_{xy}=S_{xz}=S_{yz}=0.333\ |S|$, and for $\langle 110\rangle$ stress $S_{xy}=0.5\ |S|$ and $S_{xz}=S_{yz}=0$. Note that stress of E_g symmetry has no interaction with the off-center lithium as postulated by group theory and confirmed in the experiment [8].

Appendix II

Simulation of Isotropic Strain Distribution

For "normal" lithium an isotropic distribution of strain directions is a reasonable assumption. For the numerical calculations 13 different directions have been chosen with appropriate statistical weights in order to simulate the assumed isotropy. In the stereographic projection of Fig. 9 these directions are shown. Dividing lines between the different directions were constructed analogous to the Wigner-Seitz method. The areas on the sphere correspond to the following percentages of the total space angle: 9% for each $\langle 100\rangle$, 7% for each $\langle 111\rangle$, and 7.5% for each $\langle 110\rangle$ direction. If no external fields are applied the equivalent directions are degenerate, and the total statistical weight is 27% for the three $\langle 100\rangle$, 28% for the four $\langle 111\rangle$, and 45% for the six $\langle 110\rangle$ directions.

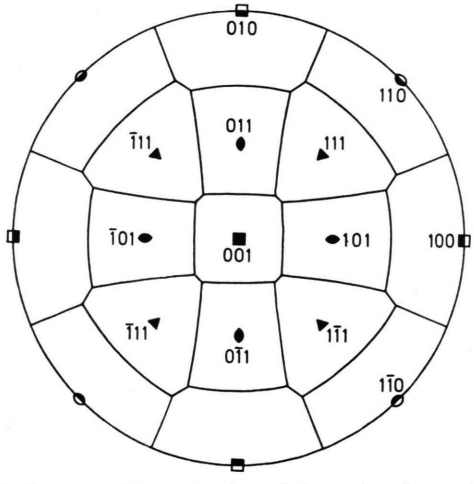

Fig. 9. Stereographic projection of the unit sphere, showing the 13 different directions which were chosen as uniaxial stress directions in the present calculation. The dividing lines between the areas were constructed in order to determine the relative statistical weights.

Appendix III

Schottky Anomaly for Tunneling Levels

If a defect center like lithium in KCl has n tunneling states and E_i is their energy difference relative to the ground state, the contribution to the specific heat, in excess to that of the host, is given by

$$\Delta c_v(T)=\frac{\partial}{\partial T}\left[\sum_{i=1}^{n}E_i\cdot\exp\{-E_i/kT\}/\sum_{i=1}^{n}\exp\{-E_i/kT\}\right].$$

This function, $\Delta c_v(T)$, vanishes for $T=0$ and $T\to\infty$ and goes through a maximum (Schottky anomaly) at a temperture $T(c_v,\max)$, which is determined by the tunneling level scheme (see Table 4). The experimental observation of the Schottky anomaly peak can therefore be used, to obtain information on the tunneling levels. However, one can not expect to gain detailed insight in a complex level scheme by the analysis of a broad peak in the specific heat. Table 4 has been prepared in order to demonstrate, what kind of information can be extracted from the experimental curve, using as few assumptions as possible, The table is organized as follows. The cases 1 through 15, with the exception of 5, 6, 7, all have $n=8$ tunneling states, grouped into two singlets and two triplets. Such a va-

Case	Energy levels (statistical weight in parenthesis) $(k_B T)$ [a]	Peak position $T(c_v,\max)$ (Δ/k_B) [a]	Peak height $c_v,\max$ (k_B) [a]
1	0 (1), Δ (3), 2Δ (3), 3Δ (1)	0.42	1.32
2	0 (1), Δ (1), 2Δ (6)	0.55	1.56
3	0 (1), Δ (1), 2Δ (3), 3Δ (3)	0.65	1.36
4	0 (1), Δ (7)	0.30	1.77
5	0 (1), Δ (3)	0.35	1.02
6	0 (1), Δ (2)	0.38	0.76
7	0 (1), Δ (1)	0.41	0.44
8	0 (3), Δ (5)	0.39	0.66
9	0 (3), Δ (4), 3Δ (1)	0.41	0.57
10	0 (3), Δ (3), 2Δ (1), 3Δ (1)	0.49	0.52
11	0 (3), Δ (1), 2Δ (3), 3Δ (1)	0.76	0.56
12	0 (1), Δ (3), 3Δ (3), 6Δ (1)	0.37	1.06
13	0 (1), Δ (3), 3/2Δ (3), 3Δ (1)	0.38	1.51
14	0 (1), Δ (3), 5/3Δ (3), 2Δ (1)	0.40	1.51
15	0 (1), Δ (3), 5/2Δ (3), 3Δ (1)	0.42	1.16
16	0, Δ, 2Δ, 3Δ, 4Δ, 5Δ (all 1)	0.84	0.85
17	35 levels from Table 3	0.43 [b]	1.11
18	density of states from Fig. 7a	0.44 [b]	1.10
—	experimental [6] (see Fig. 8)	0.49 ± 0.05 °K [c]	0.83

[a] 1 $k_B=1.3804\cdot10^{-16}$ erg/deg=20.836 GHz/deg, the normalized unit for T is Δ/k_B.

[b] Δ corresponds to center of gravity for T_{1u} derived levels (see Table 3).

[c] Measured for the natural isotopic mixture with 93% Li^7 (1 °K=0.98 Δ/k_B, see Table 3) and 7% Li^6 (1 °K=0.7 Δ/k_B).

Table 4. Calculated Schottky anomaly for a variety of level schemes.

riety of cases can arise from an ⟨111⟩ off-center ion in O_h symmetry, if only group theoretical arguments are used. Equidistant levels have been assumed for the cases 1 through 11 and non-equidistant levels for the cases 12 through 15. Each of these cases corresponds to a particular set of tunneling parameters η, μ, ν [see Eq. (3)]. Case 1 is the mostly used scheme, where $\mu=\nu=0$. Case 14 is taken from the literature [20], with $\eta:\mu:\nu=4:1:0$. Case 16 is the level scheme of WIELINGA et al. [5] which provides a satisfactory fit to the measured Schottky anomaly at very high lithium concentrations (365 ppm), if $\Delta=20.8$ GHz is assumed [5]. Cases 17 and 18, which give almost identical results, represent an ensemble of lithium ions in a KCl host with internal strains, as used in the calculation for the solid curve in Fig. 8. The last line in Table 4 gives the experimental values. Comparing calculated and observed peak heights, a triplet ground state, as assumed in the cases 8 through 11, can be ruled out. Another important result is evident for the remaining cases with a singlet ground state: the peak position is almost entirely determined by the spacing of the two lowest levels (cases 1, 4–7, and 12–15) with very little influence from the higher levels, unless the statistical weight is concentrated in these higher levels (cases 2, 3, 11, and 16). For example, a discrimination between the cases 1 and 14 is not posible from the specific heat experiment, however case 14 can be ruled out by phonon spectrometer results (see Sect. 3.1).

Appendix IV

Level Scheme for Lithium in Anomalous Sites

It is assumed that the "anomalous" lithium sites are close to dislocation lines. In alkali halides like KCl, ⟨110⟩ is the preferred direction of edge dislocations. The disturbance of the lattice in the planes perpendicular to the dislocation line is shown schematically in Fig. 10. The situation can be obtained by insertion of a string of K and Cl ions into an undisturbed layer along the line CD. The corresponding Burgers vector is shown at BB′. To the left of the line ADF, the lattice experiences a ⟨110⟩ compression, which goes to zero

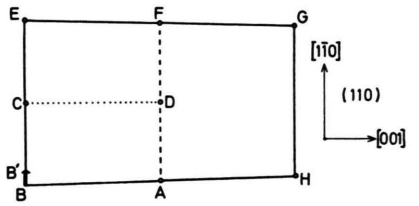

Fig. 10. Schematic representation of a (110) plane in KCl, perpendicular to a [110] edge dislocation line, which penetrates at D. The Burgers vector BB′ points in the [1$\bar{1}$0] direction. Along the lines ABEFGHA, the ions have their normal distance. This is not true along the line ADF.

at BE. To the right of ADF a ⟨110⟩ dilation occurs, which goes to zero at GH. The lithium will find shallow or no stable off-center positions in the compressed region ABEF and therefore prefer the dilated region AFGH. There, as a consequence of the lattice widening, the minima are probably deeper than in the undisturbed lattice. To obtain the corresponding tunneling levels the left part of Fig. 5 has to be extrapolated to very large stress values. The higher levels are then very far away and can be neglected. Thus, the effective level scheme consists of a ground state doublet ($A_{1g}+B_{1u}$, degenerate) and an excited tunneling doublet ($B_{3u}+B_{1g}$, degenerate). For the specific heat this is equivalent to case 7 in Table 4. The spacing is slightly larger than for normal lithium (see Fig. 5) and the ratio Δ(anomalous) : Δ(normal) = 1.2 : 1 as obtained from the fit to the Schottky anomaly in section 3 appears reasonable. It must be emphasized that this picture of the anomalous lithium is based on several assumptions and still rather incomplete. Predictions about the width of the tunneling levels can not be made.